

# A New Passive Device to Suppress Several Instabilities in Turbomachines by Use of J-Grooves

Junichi KUROKAWA, Sankar Lal SAHA, Jun MATSUI and Takaya KITAHORA

Dept. of Mechanical Engineering, Yokohama National University,  
156 Tokiwadai, Hodogaya-ku, Yokohama, Japan

## ABSTRACT

*In order to control and suppress several anomalous phenomena, such as a rotating stall in a vaneless or a vaned diffuser of a radial flow turbomachine, performance instability with a positive gradient of head-capacity curve in a mixed flow turbomachine and a draft tube surge in a Francis turbine, a new passive device using shallow grooves on a casing wall is proposed and its effect is studied experimentally. The results show that the shallow grooves with adequate dimensions can suppress these instabilities.*

*Theoretical consideration has revealed that a remarkable effects of shallow grooves are caused by two mechanisms; one is a significant decrease in the tangential velocity due to mixing between the main flow and the groove flow, and the other is an increase in meridional velocity of the main flow due to the reverse flow in the grooves.*

## 1. INTRODUCTION

Radial grooves mounted on a stationary wall have a remarkable effect of reducing the swirl of rotational flow. Even if the grooves are very shallow with only 1 mm in depth, they can reduce the swirl considerably. One of the present authors has revealed the mechanism of reducing the swirl theoretically and experimentally<sup>(1)</sup>.

It is then predicted that the method utilizing this mechanism could be one possible way of controlling and suppressing several anomalous phenomena caused by a rotational flow, such as a rotating stall in a vaneless or a vaned diffuser, performance instability with a drooping head-capacity curve and a draft tube surge, since these unstable phenomena occur in a relatively small discharge range with large swirl velocity.

As for a rotating stall in a vaneless or a vaned diffuser, many studies have been performed so far<sup>(2)-(5)</sup> and the method of suppressing this unstable phenomenon has long been pursued. However, most of the methods so far proposed require complicated mechanisms, and it is as yet a strong requirement to find a simple method of suppressing a rotating stall. The present authors have revealed that the radial shallow grooves mounted on a diffuser wall is very effective to suppress a rotating stall in a vaneless or a vaned diffuser<sup>(6)</sup>.

Performance instability characterized by a positive gradient of the head-capacity curve sometimes causes severe pressure oscillation. To suppress this phenomena an active control using jet injection was proposed<sup>(7)</sup>. As this phenomena

is caused by a sudden drop of theoretical head due to strong swirl of the reverse flow at an impeller inlet<sup>(8)</sup>, it should also be possible to suppress this instability by the grooves.

A draft tube surge in a Francis turbine induces severe power swing in an electric generating system, and is caused by a swirl flow at the exit of a Francis runner. To suppress the swirl a method using ribs was proposed<sup>(9)</sup>. The grooves should also be very effective to suppress the swirl of a runner outlet flow.

The present study is thus aimed to reveal the effects of shallow grooves mounted on the casing wall upon the anomalous phenomena caused by a swirl flow. As a strong flow is induced in the shallow grooves due to a pressure gradient, it is of key importance to provide the grooves perpendicular to the pressure gradient. Here we call such shallow grooves mounted perpendicular to the pressure gradient as "J-grooves".

In the first step of the present study, the mechanism of suppressing the swirl is elucidated theoretically by use of the rotational flow in a parallel-walled vaneless diffuser. In the second step, the effects of J-grooves are shown upon suppressing a rotating stall in a vaneless and a vaned diffusers, performance instability in a mixed flow pump and a swirl flow in a conical diffuser.

## 2. WHAT HAPPENS BY J-GROOVES ?

To elucidate the mechanism of suppressing swirl by J-grooves, the flow in a parallel-walled vaneless diffuser is analyzed here, when radial shallow grooves are provided on a casing wall. Anomalous phenomena generally occur in the low flow range where the radial velocity  $v_r$  is much smaller than the tangential velocity  $v_\theta$ . Supposing  $v_r \ll v_\theta$  in the vaneless diffuser with radial grooves, the equations of angular momentum balance, momentum balance and of continuity are written as follows referring to Fig. 1:

$$d/dr[2\pi\rho r^2 b \overline{v_r \overline{v_\theta}}] - \rho r \overline{v_\theta} (dQ_G/dr) = -4\pi r^2 \tau_\theta \quad (1)$$

$$dp/dr = \rho \overline{v_\theta}^2 / r \quad (2)$$

$$2\pi r b \overline{v_r} = Q \quad (3)$$

where the bar denotes the averaged value over the section from the upper wall  $z=0$  to the lower  $z=b$ , and the double bar denotes the mass-averaged one.  $Q_G$  is the flow rate in the grooves. The second term in the left hand of Eq. (1) represents the angular momentum lost by the flow coming into the groove.

The groove flow is driven by radial pressure gradient and the balance of forces in the groove is expressed as

$$A dp = \tau_0 s dr, \quad (4)$$

where  $A$  and  $s$  are the sectional area and the wetted surface length of the groove, respectively. The wall shearing stress terms  $\tau_\theta = C_f \rho v_{\max} v_{\theta \max} / 2$  in Eq. (1) and  $\tau_0$  in Eq.(4) on the groove wall are given as a function of flow angle  $\alpha$  and the tangential velocity  $v_\theta^{(6)}$ .

Finally the non-dimensional tangential velocity  $V_\theta = \bar{v}_\theta / u_z$  is obtained numerically as a function of radius ratio  $R = r/r_2$ , when the boundary value  $V_{\theta 2}$  at  $R=1.0$  is given. The groove flow comes inward in the groove and mixes with the main flow at diffuser inlet resulting in a sudden drop of  $V_{\theta 2}$ . Supposing that the main flow  $Q$  and the groove flow  $Q_G$  soon mix to be uniform in the small region  $\Delta r$ , the angular momentum balance determines the boundary value  $V_{\theta 3} (= \bar{v}_{\theta 3} / u_z)$  at  $R=1+\Delta r/r_2$  by

$$\rho r_2 \bar{v}_{\theta 2} Q = \rho r_3 \bar{v}_{\theta 3} (Q + Q_G) + 2 \int_{r_2}^{r_2 + \Delta r} 2\pi r^2 \tau_\theta dr \quad (5)$$

The calculated results are illustrated in Figs. 2 and 3 at  $R=1.0$  by comparing with the measured ones. The change of flow angle  $\alpha$ , defined as  $\alpha = \tan^{-1}(\bar{v}_r / \bar{v}_\theta)$ , is plotted in Fig. 2 against the discharge coefficient  $\phi = Q / (2\pi r_2 b \mu_2)$  for three cases, the no groove case ( $\bullet$ ), the grooved case of 1 mm depth on both walls ( $\square$ ) and that of 3 mm depth on the upper wall ( $\Delta$ ).

Figure 2 shows that the flow angle  $\alpha$  increases considerably by use of radial grooves of only 1 mm depth over all discharge ranges, and that the groove effect increases with a decrease in  $\phi$ . Here it is to be remarked from the measured data that the 1 mm-depth groove on both walls has almost the same effect as the 3 mm-depth groove on one sidewall.

If the increase of  $\alpha$  were caused only by the decrease of tangential velocity, it would become much smaller than that shown in Fig. 2. This means that the radial velocity  $v_r$  also increases largely. To show this more clearly, the flow rate ratio  $Q_G/Q$  of the groove flow to the main flow at  $R=1.10$  are illustrated in Fig. 3. It is surprising that the flow rate amounts to more than 40% of the main flow in the shallow grooves of 3 mm depth in the low flow range. The contribution of the mixing of the main flow with the groove flow is further estimated. The increase of  $\alpha$  then becomes half of the total increase of  $\alpha$ .

Accordingly, it is concluded that the remarkable effects of radial grooves are caused by the following two mechanisms; one is a remarkable decrease of tangential velocity at the diffuser inlet due to the mixing between the main flow and the groove flow, and the other is a remarkable increase of radial velocity due to the reverse flow in the grooves. Both the effects have the same weight of contribution to increase the flow angle. Even if the groove is very shallow such as  $d=1$  mm, the increase of flow angle is very large near the wall.

### 3. SUPPRESSION OF ROTATING STALL

To confirm the validity of J-grooves on suppressing a rotating stall, two kinds of tests were conducted. One is the

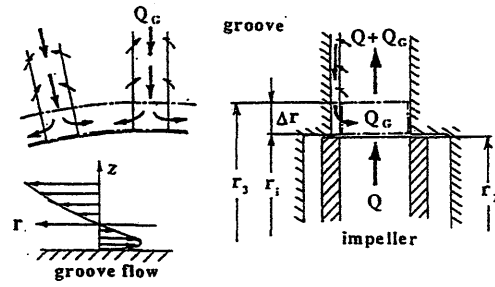


Fig. 1 Notations and the flow in a radial groove

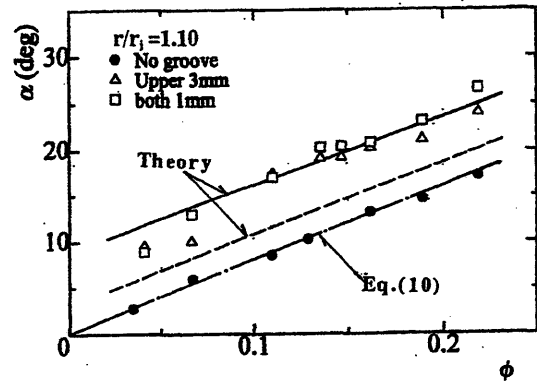


Fig. 2 Mean flow angle vs. discharge coefficient  $\phi$

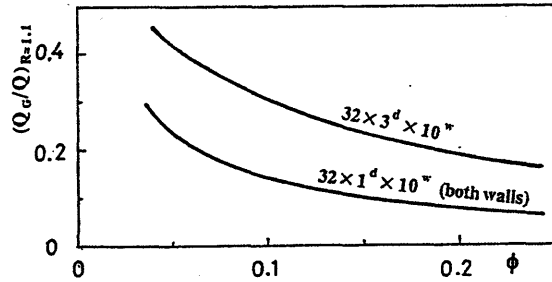
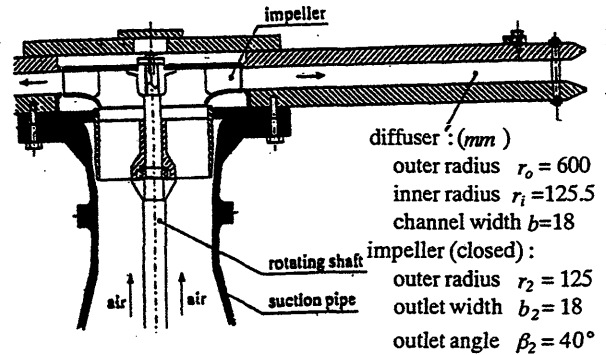


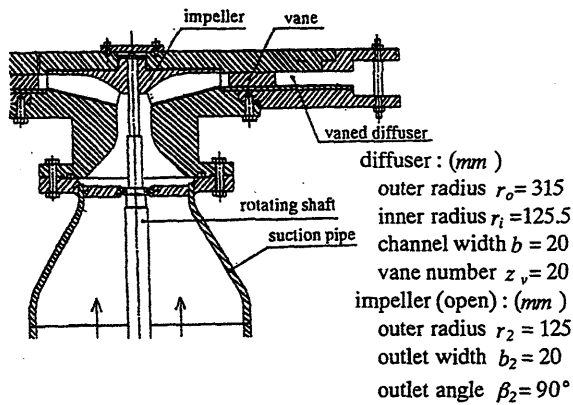
Fig. 3 Flow rate ratio of groove flow to main flow



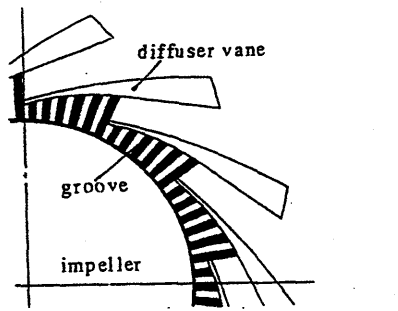
(a) Vaneless Diffuser test stand  
Fig. 4 Test stand of rotating stall

vaneless diffuser test and the other is the vaned diffuser test, of which test stands are shown in Figs. 4 (a) and (b).

The impeller outlet width  $b_2$  is equal to the diffuser width  $b$ . A supplemental blower is set at the upstream to control



(b) Vaned Diffuser test stand



(c) Diffuser vanes and radial grooves  
Fig. 4 Test stand of rotating stall

the flow rate widely. In the vaneless diffuser test the vane angle  $\beta_v$  is varied from  $\beta_v = 8^\circ$  to  $\beta_v = 16^\circ$  and the vane configuration is illustrated in Fig. 4 (c).

The radial grooves used in the vaneless diffuser tests are of the width  $w=10$  mm, the depth  $d=1$  or  $3$  mm and the number of grooves  $n$  is varied from 4 to 32. The groove length is equal to  $(r_o-r_i)$  and short grooves of 50, 70 and 125 mm in length are also tested. In the vaneless diffuser test two kinds of radial grooves are used, the grooves of  $n=78$ ,  $w=5$  mm,  $d=3$  mm and those of  $n=39$ ,  $w=5$  mm,  $d=3$  mm. In both tests the impeller speed is 3000 rpm, and the corresponding Reynolds number  $Re \equiv u_2 r_2 / \nu$  is  $3.3 \times 10^5$ .

### 3.1 Rotating Stall in a Vaneless Diffuser

The wall pressure fluctuations measured at  $R=r/r_i=1.10$  in the vaneless diffuser are plotted in Fig. 5, when there is no J-grooves.

With a decrease in the flow angle  $\alpha$ , a periodical pressure fluctuation initiates at  $\alpha = 26^\circ$ , corresponding to  $\phi = 0.33$ . This fluctuation grows to a clear sinusoidal oscillation as shown in Fig. 5(a). The pressure data revealed that this oscillation is the rotating stall with two cells. With further decrease in  $\alpha$ , both the frequency and the amplitude increase (Figs. 5(b) and (c)), and the oscillation changes from sinusoidal to triangular superimposed with higher harmonic waves. The amplitude of two-cell-oscillation takes the maximum near  $\alpha=15^\circ$  and decreases with further decrease in  $\alpha$ . Around  $\alpha=12^\circ$ , another oscillation with much lower frequency with one cell is imposed to two-cell-oscillation (Figs. 5(d) and (e)).

With further decrease in  $\alpha$ , the one-cell-oscillation

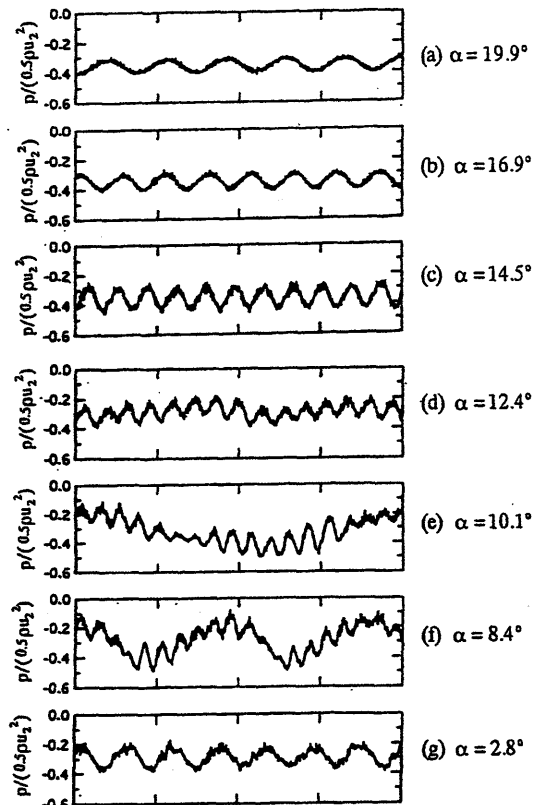


Fig. 5 Rotating stall in the vaneless diffuser of  $r_o/r_i=4.78$

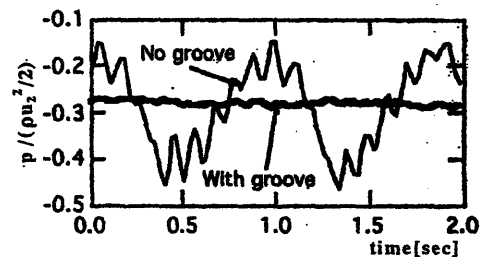


Fig. 6 Effect of radial grooves on suppressing rotating stall in vaneless diffuser (grooves:  $32^n \times 3^d \times 10^w$ )

becomes prominent ( Figs. 5(e) and (f) ), and grows to a large pressure fluctuation. The amplitude amounts to about twice that of two-cell-oscillation. The frequency increases with a decrease in  $\alpha$  until  $\alpha=5^\circ$  and then decreases as shown in Fig. 5(g), while the amplitude of two-cell-oscillation decreases monotonously and disappears. In the range of  $\alpha < 2^\circ$  the rotating stall disappears.

### 3.2 Suppression of Rotating Stall in a Vaneless Diffuser

To suppress a rotating stall in a vaneless diffuser, several kinds of radial grooves were tested.

The number  $n$  of grooves was increased for the fixed depth of  $d=3$  mm and the width of  $w=10$  mm. With an increase in  $n$  from 4, the amplitude of pressure fluctuation decreased remarkably and the flow rate range of rotating stall also decreased largely. But it was not until  $n=32$  that the stall was

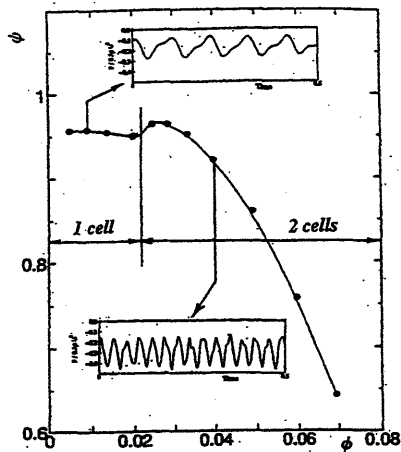


Fig. 7 Performance curves when the vanes are removed

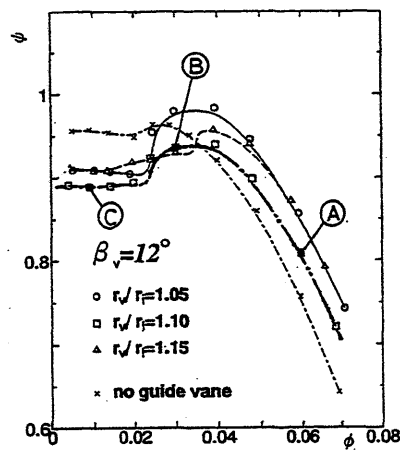


Fig. 8 Performance curves and rotating stall in a vaned diffuser

completely suppressed over the whole flow range. As an example, the wall pressure fluctuation measured at  $R = 1.10$  is compared with the no-grooved case in Fig. 6. This is the case of the largest pressure fluctuation shown in Fig. 5. It is clearly seen that the periodic pressure fluctuation is completely suppressed by the grooves.

Several grooves with various dimensions were tested and it was revealed that the groove dimensions which could suppress the rotating stall completely in all flow ranges were  $32^d \times 3^m \times 10^w$  on one sidewall and  $32^d \times 1^m \times 10^w$  on both sidewalls. The larger dimensions than those suppress rotating stall completely.

The short grooves were also tested and the results shows that they can also suppress a rotating stall remarkably. For example, the grooves of 50 mm in length and of  $32^d \times 3^m \times 10^w$  on one sidewall reduces the range of rotating stall from  $\alpha \leq 26^\circ$  to  $\alpha \leq 7^\circ$  and the amplitude to a half. Although they could not suppress a rotating stall completely, yet they were very effective.

### 3.3 Suppression of Rotating Stall in a Vaned Diffuser

To show the effects of diffuser vane, the vanes were removed, and the head-capacity curve is shown in Fig. 7, in which the pressure fluctuation measured at  $r/r_i = 1.10$  is also illustrated. A typical rotating stall for a vaneless diffuser is observed over all discharge ranges and the head curve shows a rapid drop around  $\phi = 0.02$  at which two-cells oscillation suddenly changes to one-cell oscillation with a decrease in  $\phi$ .

When the diffuser vanes are mounted, a rotating stall does not occur in the case of the vane angle  $\beta_v = 16^\circ$ , but occurs in  $\beta_v = 12^\circ$  and  $8^\circ$ . Here, the radius  $r_v$  of the vane leading edge is varied and the change of head curve is compared in the case  $\beta_v = 12^\circ$  in Fig. 8, where four cases,  $r_v/r_i = 1.05$ , 1.10 and 1.15 and the vaneless case, are compared. In the right of Fig. 8 is illustrated the pressure fluctuation in the case of  $r_v/r_i = 1.10$  for three operating points A, B and C.

Comparison with the vaneless case reveals that the total pressure increases by use of diffuser vanes in the large discharge range. But with a decrease in the discharge  $\phi$  the total

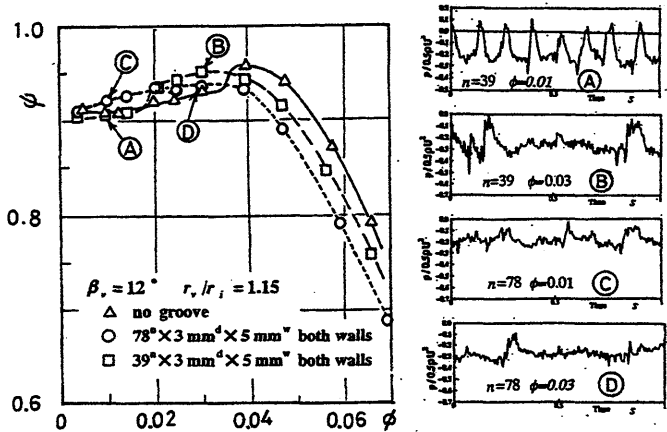
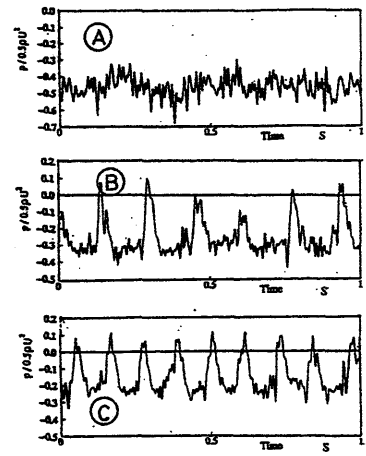


Fig. 9 Suppression of rotating stall in a vaned diffuser

pressure drops rapidly, when the rotating stall initiates with a triangular pressure fluctuation (B) typical for a vaned diffuser. In this case the total pressure becomes lower than the vaneless case. With further decrease in  $\phi$  the amplitude of the pressure fluctuation shows no change and the frequency increases a little as shown in (C). It is also recognized that the discharge at a rapid head drop decreases with a decrease in the vane leading edge radius  $r_v$ .

To suppress the rotating stall, two kinds of J-grooves are used as shown in Fig. 4(c). The change of performance curves is shown in Fig. 9, in the right of which the pressure fluctuations for  $\beta_v = 12^\circ$  and  $r_v/r_i = 1.15$  are also illustrate at four operating points A, B, C and D indicated in the head curve.

It is clearly seen that the rapid head drop disappears in the case of  $n=78$  in all flow ranges, and that the discharge at the sudden head drop decreases to a half in the case of  $n=39$ . In the latter case the periodical fluctuation still exists at a very low discharge. It is also recognized that a complete suppression of a rotating stall requires an increase of hydraulic loss by about 7% of  $\rho u_2^2/2$  or by about 8% of the total pressure in the large discharge range.

In a practical use, it is not always necessary to suppress a rotating stall in all flow ranges, as the flow phenomena often

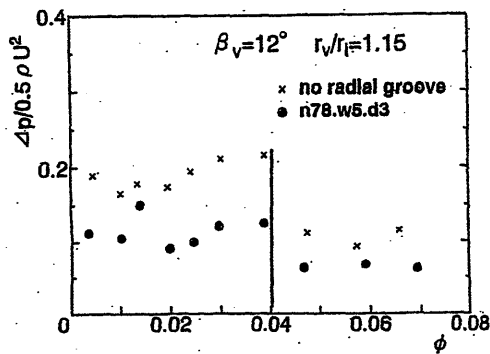


Fig. 10 Reduction of pressure fluctuation by J-grooves

changes from a rotating stall to a surge in a very low flow range in blowers and compressors or there is a requirement of minimum flow in pumps. In such cases much smaller number of grooves is enough and head loss decreases.

Another advantage of J-grooves is that they can reduce a pressure fluctuation in all flow ranges. The peak-to-peak amplitude of the periodic or random pressure fluctuation is illustrated in Fig. 10. It is recognized that J-grooves can reduce the pressure fluctuation to about a half in all flow ranges including the flow range of non-rotating stall.

#### 4. IMPROVEMENT OF PERFORMANCE INSTABILITY IN A MIXED FLOW PUMP

The J-grooves are applied to improve the performance instability with positive slope of head-capacity curve in a mixed flow pump, as a sudden drop of head curve is mainly caused by a strong swirl of the reverse flow at an impeller inlet. In order to produce a groove flow, the J-grooves are mounted parallel to the impeller axis on a casing wall, and the axial pressure gradient created by an impeller is utilized. It is then expected that the groove flow should suppress a swirl of the impeller inlet reverse flow at low discharge range and should give no influence on the pump performance at high discharge range.

The mixed flow pump used for this purpose is shown in Fig. 11. The specific speed  $N_s$  is 860 [ $m, m^3/min, rpm$ ], the tip clearance is 0.7 mm and a swirl stop is mounted at the impeller upstream. As the dimensions of the groove including the position influence the performance instability much, several dimensions were tested. The optimum groove dimensions experimentally determined are illustrated in Fig. 12.

The comparison of the test results are illustrated in Fig. 13 for three cases, the no groove case, the grooved case of  $28^h \times 4^d \times 5^w$  mm and that of  $28^h \times 2^d \times 10^w$  mm. In the no groove case (○), unstable performance with rapid drop of head curve is clearly seen at  $\phi=0.13$ . But a considerable improvement is attained, when the grooves of  $28^h \times 2^d \times 10^w$  mm (□) are mounted around the impeller inlet region on the casing wall. No positive slope in head-capacity curve is seen in the whole discharge range. It is also recognized that this device does not create any additional hydraulic loss, which results in that the efficiency increases at the discharge of the rapid head drop and that the maximum efficiency is not influenced by the

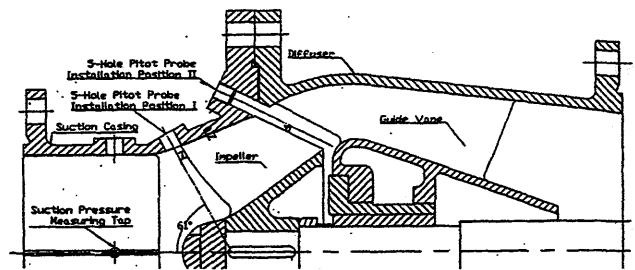


Fig. 11 Mixed flow pump tested ( $N_s=860$ )

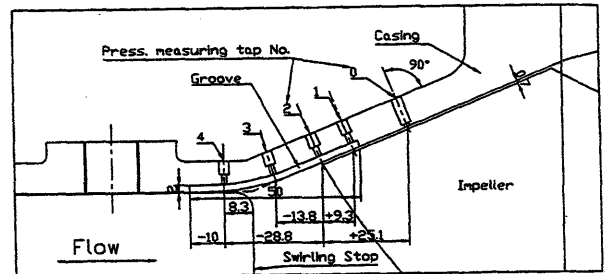


Fig. 12 J-Grooves mounted on a casing wall

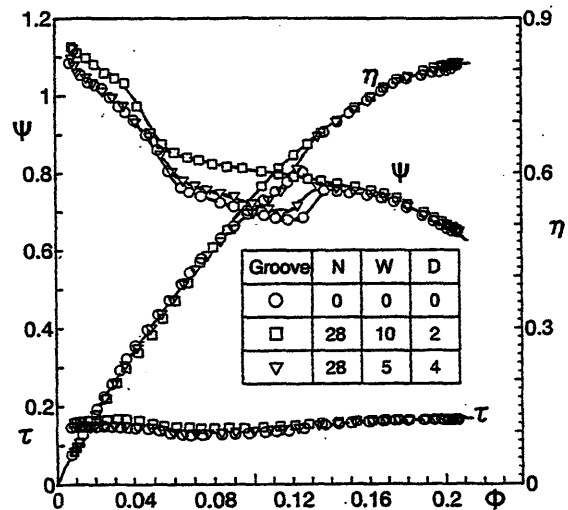


Fig. 13 Improvement of performance instability

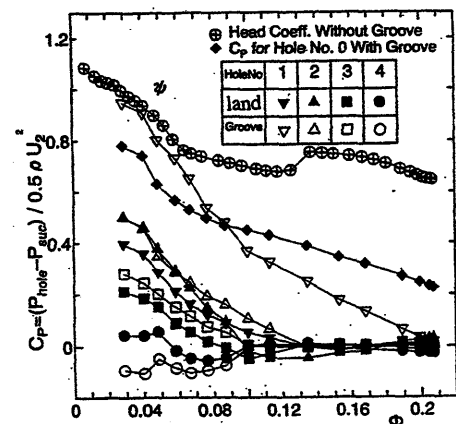


Fig. 14 Pressure changes at the measuring hole No. 1-4

grooves. In the grooved case of  $28^{\text{n}} \times 4 \text{ mm}^{\text{d}} \times 5 \text{ mm}^{\text{w}}$  ( $\nabla$ ), only a little improvement is attained but large instability still remains, though the total sectional area of the groove is same in both cases. This reveals that the width of the groove is of key importance.

The above remarkable improvement of the head-capacity curve is attained by a considerable decrease of both the swirl strength of the inlet reverse flow and the size of the reverse flow region near the tip of an impeller inlet, which are caused by the groove flow with no swirl.

To reveal the behavior of the groove flow, the pressure change along the wall is shown in Fig. 14, in which two kinds of pressure data are shown, the pressure at the bottom of the groove and that at the surface of the wall (land). The hole number in Fig. 14 corresponds to that shown in Fig. 12 and the pressure coefficient  $C_p$  is defined by the non-dimensional pressure difference ( $p_{\text{hole}} - p_{\text{suc}}$ ).

It is recognized that the pressure at No. 1 hole in the groove is extremely high in the low discharge range. The pressure in the other holes show slight difference in the stable performance range ( $\phi > 0.13$ ). However, when the performance instability occurs at  $\phi = 0.13$ , the pressure rises rapidly from No. 4 to 1 in the main flow direction, and the groove flow should be induced by this pressure gradient. As this groove flow is reverse to the main flow, it makes the impeller inlet reverse flow disappear. With further decrease in discharge, the pressure gradient becomes considerable and a strong groove flow should be induced.

## 5. SUPPRESSION OF SWIRL IN A CONICAL DIFFUSER BY USE OF J-GROOVES

In order to develop a passive control method of suppressing a draft tube surge, the effect of J-grooves on the swirl flow in a conical diffuser is studied by use of the test apparatus shown in Fig. 15. The swirl flow is produced by an axial flow impeller set just before the divergent channel. The supplemental blower is arranged at far upstream of the divergent channel to change the flow rate widely.

The angle of divergence  $\alpha_p$  of the conical diffuser is selected to  $30^\circ$  and the ratio of the sectional area  $(D_2/D_1)^2$  is 3.84. The J-grooves are provided by attaching the rectangular thin plates of  $30^{\text{n}} \times 4 \text{ mm}^{\text{d}} \times 5 \text{ mm}^{\text{w}}$  over the whole wall of the divergent channel, and then the groove dimensions are  $30^{\text{n}} \times 4 \text{ mm}^{\text{d}} \times 11.3 \text{ mm}^{\text{w}}$  at the inlet of the divergent channel and  $30^{\text{n}} \times 4 \text{ mm}^{\text{d}} \times 26.9 \text{ mm}^{\text{w}}$  at the outlet.

The velocity distributions at four sections shown in Fig. 15 are measured by a 3-hole Pitot probe set perpendicular to the wall. The wall pressure distribution was also measured at 5 points in the streamwise direction. The test Reynolds number  $Re = V_1 D_1 / \nu$  based on the inlet axial velocity  $V_1$  and the diameter  $D_1$  is  $(1.0 \sim 3.0) \times 10^5$ .

Two kinds of swirl strength are selected to reveal the effect of J-grooves by setting the impeller speed to 305 rpm and 730 rpm under the constant flow rate. The corresponding swirl strength  $m$  defined by the following equation is 0.45 and 0.93, respectively.

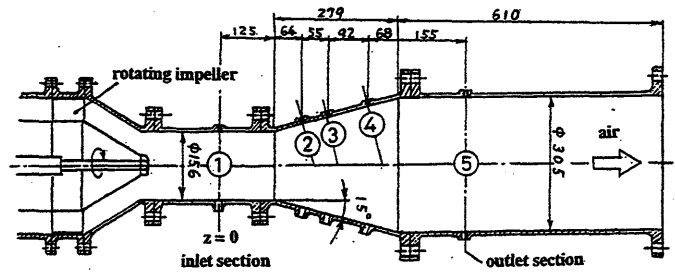


Fig. 15 Conical diffuser test stand

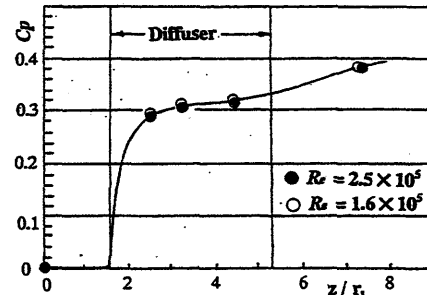


Fig. 16 Pressure rise in the flow direction

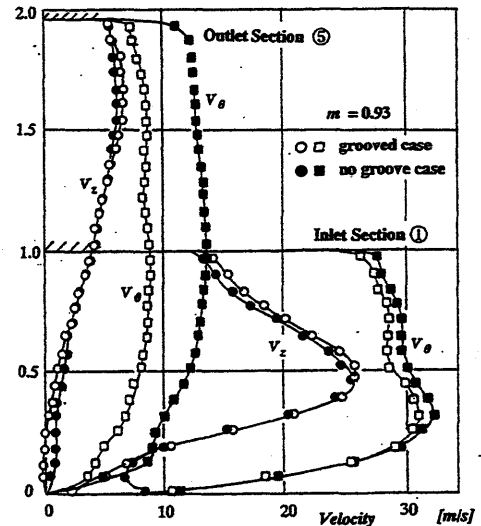


Fig. 17 Suppression of swirl by J-grooves

$$m = \frac{\int v_z v_\theta r dA}{\int v_z^2 r dA} \quad (5)$$

Here,  $v_z$  and  $v_\theta$  are the axial and the swirl velocity components, respectively, and  $A$  is the sectional area.

The pressure distribution along the diffuser wall is shown in Fig. 16 in the case of no swirl. It is recognized that the pressure recovers not only in the divergent channel but also in the downstream pipe. This reveals that a large separation occurs in the divergent channel and the separation zone elongates to the downstream pipe where significant pressure recovery is attained.

When a swirl is given by an impeller, the velocity distribution in the inlet section changes remarkably and the wall

pressure changes considerably depending on the swirl strength. The measured velocity profiles in the inlet section ① and that at the outlet section ⑤ are compared in Fig. 17 in the case of  $m=0.93$  (0.96 in the no groove case and 0.89 in the grooved case). In the inlet section the low axial velocity zone is formed around the channel axis. In Fig. 17 is also shown the velocity profiles of the grooved case. Comparison of the no groove case with the grooved case reveals that the swirl strength is largely suppressed over the whole area at the outlet section by attaching the J-grooves.

But in the divergent channel the velocity profile is not so uniform in both cases as illustrated in Fig. 18. This figure shows the velocity distribution in the case of  $m=0.93$  measured at the section ④, which is perpendicular to the wall and not to the axis. The velocity profile in Fig. 18 reveals that the swirl velocity  $v_\theta$  is suppressed to about 60% by J-grooves over the whole section, and the velocity  $v_m$  parallel to the wall shows the existence of a large reverse flow region in the center. This reverse flow region becomes stronger in the grooved case, but it hardly elongates to the down stream.

## 6. CONCLUSIONS

A new passive device using J-grooves is proposed to suppress several anomalous phenomena caused by a swirl flow in a turbomachine, such as a rotating stall in vaneless and vaned diffusers, performance instability with positive slope of head-capacity curve and a draft tube surge. Remarkable effects of suppressing these phenomena are confirmed experimentally, though the mechanism is not yet fully elucidated.

The main conclusions are summarized as follows;

- (1) Though the shallow radial grooves are very simple, the effect of decreasing the flow angle is conspicuous in a parallel-walled diffuser. Using the groove dimensions of  $32^\circ \times 3^d \times 10^w$  on one sidewall or  $32^\circ \times 1^d \times 10^w$  on both walls, a rotating stall in a vaneless diffuser is completely suppressed in all flow ranges. A rotating stall in a vaned diffuser is also suppressed completely in almost all flow ranges using the short grooves of  $78^\circ \times 3^d \times 5^w$ . The decrease in the tangential velocity necessarily accompanied with the decrease in total pressure.
- (2) The shallow grooves are also very effective to improve performance instability with a positive slope of head-capacity curve. When the J-grooves of proper dimensions are mounted properly on the casing wall of a mixed flow pump, the performance instability can be removed perfectly with an efficiency increase, and the maximum efficiency does not decrease at all.
- (3) The J-grooves can suppress the swirl strength of a rotational flow in a conical diffuser. The measured results revealed that it decreases the swirl strength to about 60 % of the no-groove case under the condition of the divergent angle  $\alpha_D=30^\circ$  and the swirl strength  $m=0.93$ .

## ACKNOWLEDGEMENT

The present work was supported by the Ministry of

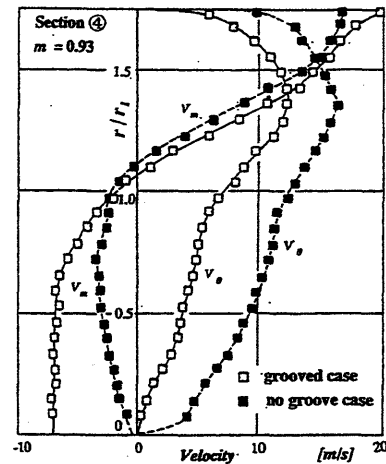


Fig. 18 Velocity profile in the section ④

Education, Science, Sports and Culture under Grant-in-Aid for Scientific Research Nos. 06555054 (1994) and 09555062 (1997).

## REFERENCES

- (1) Kurokawa, J., Kamijo, K. and Shimura, T., Axial Thrust Behavior in LOX-Pump of Rocket Engine, *AIAA, Jr. Propulsion and Power*, Vol. 10 No. 2(1994), pp. 244-250.
- (2) Jansen, W., Rotating Stall in a Radial Vaneless Diffuser, *Trans. ASME, Jr. Basic Engineering*, Vol. 86, No. 4(1964), pp. 750-758.
- (3) Senoo, Y. and Kinoshita, Y., Limits of Rotating Stall in Vaneless Diffuser of Centrifugal Compressors, *ASME Paper* No. 78-GT-19(Apr. 1978).
- (4) Tsurusaki, H., Effects of Diffuser Geometry on Rotating Stall in Vaneless Diffuser, *Trans. JSME (in Japanese)*, Vol. 59, No. 566(1993), pp. 3133-3139.
- (5) Yosida, Y., Murakami, Y., Tsurusaki, H. and Tsujimoto Y., Rotating Stall in Centrifugal Impeller/Vaned Diffuser Systems, *Proc. ASME-JSME Joint Conf. (Portland)*, FED-Vol.107(1991).
- (6) Kurokawa, J., Saha, S. L., Matsui, J. and Kitahara, T., A New Passive Control of Rotating Stall in Vaneless and Vaned Diffusers By Shallow Grooves, *Proc. JSME Sympo.*
- (7) Goto, A., Suppression of Mixed-Flow Pump Instability and Surge by the Active Alteration of Impeller Secondary Flows., *Trans. ASME, Jr. of Turbomachinery*, Vol. 116 (1994-Oct.), pp.621-628.
- (8) Kurokawa, J. and Juang, J., Performance Prediction of a Mixed-Flow Pump, *Bulletin JSME*, Vol.28, No.241 (1985), pp. 1423-1429.
- (9) Nishi, M., Wang, X. M., Yoshida, K., Takahashi, T. and Tsukamoto, T., An Experimental Study on Fins, Their Role in Control of the Draft Tube Surging, *Proc. 18th IAHR Symposium on Hydraulic Machinery and Cavitation (Valencia)*, Vol.2 (1996), pp.905-914.